



## STEEL FRAME / WOOD PANEL SHEAR WALLS : PRELIMINARY DESIGN INFORMATION FOR USE WITH THE 2005 NBCC

C.A. ROGERS<sup>1</sup>, A.E. BRANSTON<sup>2</sup>, F.A. BOUDREAU<sup>2</sup>, C.Y. CHEN<sup>2</sup>

### SUMMARY

It is anticipated that the construction of homes and multiple storey buildings which incorporate light gauge steel frame / wood panel shear walls will increase across Canada in coming years. This includes sites that have a relatively high seismic risk, such as found along the West Coast of British Columbia and in the Ottawa and St. Lawrence River Valleys. Currently, guidelines for engineers with which the design of laterally loaded steel frame / wood panel shear walls can be carried out are not available in Canada. For this reason an extensive shear wall research program has been undertaken at McGill University. The long-term objective of this research is to develop guidelines for the seismic design of steel frame / wood panel shear walls for use with the 2005 National Building Code of Canada (NBCC). This paper presents the preliminary findings of 106 tests of walls constructed with Canadian sheathing products (12.5 mm Douglas Fir Plywood, 12.5 mm Canadian Softwood Plywood and 11 mm Oriented Strand Board) and steel products (1.1 mm 230 MPa) following the limit states design philosophy required by the National Building Code. Information will be provided on the results of the test program, as well as on the general approach used for the interpretation of monotonic and reversed cyclic test data in developing shear wall nominal capacity and stiffness values.

### INTRODUCTION

The use of light gauge steel framing as the primary load carrying element in a structure is becoming more common across North America. With this rise in construction activity comes an accompanying increase in the probability that a light gauge steel frame structure will be subjected to the demands of a severe earthquake. At present, no document exists in Canada with which engineers can design steel frame / wood panel shear walls subjected to lateral loading. The general configuration of steel frame / wood panel shear walls follows, to a degree, that of wood platform frame construction. Essentially the wood studs and plates are replaced with light gauge steel equivalents, the wood sheathing remains the same, screw fasteners are used in place of nails, etc. Hence, these steel frame / wood panel shear walls share some, but not all, of their overall performance characteristics with wood walls. Noting this, the shortcomings with respect to

<sup>1</sup> Assistant Professor, Department of Civil Engineering and Applied Mechanics, McGill University, Montreal, QC, Canada

<sup>2</sup> Postgraduate Student, Department of Civil Engineering and Applied Mechanics, McGill University, Montreal, QC, Canada

wood shear walls that were identified in the aftermath of the Northridge California earthquake (January 17, 1994) could be expected to affect the performance of steel frame / wood panel shear walls. The Northridge earthquake, a major seismic event the likes of which could also occur along the West Coast of BC, resulted in US \$40 billion in property damage to wood frame construction, reduced 48,000 wood frame housing units to an uninhabitable status, and was responsible for 25 fatalities, 24 of which were caused by damage to wood frame buildings [1].

Even though steel frame and wood frame shear walls share some performance characteristics, their behaviour in the non-linear range and at the onset of failure is somewhat different. Firstly, the presence of thin shaped cold-formed steel sections introduces the possibility of compression failure in the chord studs of a shear wall. Secondly, the wood to steel screw connections do not exhibit the same behaviour as wood to wood nail connections because of the thinness of the steel framing members and the rigidity of the screw fasteners themselves. Given this variation in behaviour from wood shear walls and the fact that a design document does not exist in Canada, a research program on steel frame / wood panel shear walls was undertaken.

The objectives of the research described in this paper included: i) To carry out a suite of tests on light gauge steel / wood panel shear walls constructed of Canadian products, and ii) To establish an approach to interpret the test data such that design values can be recommended. The scope of study involved the full-scale testing of various length single-storey walls (8' (2440 mm) in height) composed of three types of wood sheathing: Douglas Fir Plywood (DFP) [2], Canadian Softwood Plywood (CSP) [3], and Performance Rated Oriented Strand Board (OSB) [4], as well as one thickness and size of ASTM A653 [5] steel framing, and self drilling / self tapping screws. Various screw fastener spacing distances were used, and in all cases, hold-downs were installed at the base of the chord studs. In total, 106 tests of shear walls subjected to lateral load only were completed. The resulting nominal strength and stiffness values would be useable under the proposed 2005 National Building Code of Canada (NBCC) [6].

## EXPERIMENTAL STUDY

### Test Program

In the summer of 2002 a frame designed specifically for the testing of shear walls was installed in the structures laboratory at McGill University. This self-equilibrating structure can be used to displace the top of a test wall while measuring the wall resistance (Figures 1&2). A 250 kN capacity dynamic actuator with a displacement range between  $\pm 125$  mm was installed in the frame to laterally displace each specimen under stroke control. The secondary column, which was designed to pivot at its base, serves two purposes: i) The column supports the weight of the actuator, thereby allowing the main component of the force transmitted to the wall to be horizontal, and ii) If needed, it also allows for the actual actuator displacement to be amplified at the top of the wall by lowering the actuator's attachment position on the column. Lateral braces prevent the out-of-plane movement of the wall while Teflon guides coated with grease ensure that friction forces are negligible. Instruments were installed to measure resistance and acceleration, as well as slip, uplift and lateral displacements (Figures 2&3).

A total of 106 steel frame / wood panel shear wall tests were carried out during the summer of 2003 (Table 1) [7,8,9]. In most cases, six specimens (3 monotonic and 3 reversed cyclic) were tested per wall configuration to provide a minimum level of validity/reliability for the test data, however, when the initial series of tests exhibited large variation ( $> 10\%$ ), it was deemed necessary to perform supplementary tests. The test matrix included three wall specimen sizes: 2'  $\times$  8' (610  $\times$  2440 mm), 4'  $\times$  8' (1220  $\times$  2440 mm) and 8'  $\times$  8' (2440  $\times$  2440 mm), as well as different combinations of the following materials and components:

**Table 1: Light gauge steel frame / wood panel shear wall test program matrix**

Specimen	Protocol	Wall Length (ft)	Wall Height (ft)	Sheathing Type	Sheathing Thickness (mm)	Fastener <sup>4</sup> Schedule (in)
1 – A,B,C	Monotonic	4	8	CSP	12.5	4/12
2 – A	Cyclic <sup>1</sup>	4	8	CSP	12.5	4/12
3 – A,B,C	SPD <sup>2</sup>	4	8	CSP	12.5	4/12
4 – A,B,C	CUREE <sup>3</sup>	4	8	CSP	12.5	4/12
5 – A,B,C,D	Monotonic	4	8	DFP	12.5	4/12
6 – A,B,C	CUREE	4	8	DFP	12.5	4/12
7 – A,B,C	Monotonic	4	8	CSP	12.5	6/12
8 – A,B,C	CUREE	4	8	CSP	12.5	6/12
9 – A,B,C	Monotonic	4	8	CSP	12.5	3/12
10 – A,B,C	CUREE	4	8	CSP	12.5	3/12
11 – A,B,C	Monotonic	4	8	DFP	12.5	6/12
12 – A,B,C	CUREE	4	8	DFP	12.5	6/12
13 – A,B,C	Monotonic	4	8	DFP	12.5	3/12
14 – A,B,C,D	CUREE	4	8	DFP	12.5	3/12
15 – A,B,C	Monotonic	2	8	CSP	12.5	6/12
16 – A,B,C	CUREE	2	8	CSP	12.5	6/12
17 – A,B,C	Monotonic	2	8	CSP	12.5	4/12
18 – A,B,C	CUREE	2	8	CSP	12.5	4/12
19 – A,B,C	Monotonic	2	8	OSB	11	6/12
20 – A,B,C	CUREE	2	8	OSB	11	6/12
21 – A,B,C	Monotonic	4	8	OSB	11	6/12
22 – A,B,C	CUREE	4	8	OSB	11	6/12
23 – A,B,C	Monotonic	4	8	OSB	11	4/12
24 – A,B,C	CUREE	4	8	OSB	11	4/12
25 – A,B,C	Monotonic	4	8	OSB	11	3/12
26 – A,B,C	CUREE	4	8	OSB	11	3/12
27 – A,B,C	Monotonic	2	8	OSB	11	4/12
28 – A,B,C	CUREE	2	8	OSB	11	4/12
29 – A,B,C	Monotonic	8	8	CSP	12.5	6/12
30 – A,B,C	CUREE	8	8	CSP	12.5	6/12
31 – A,B,C,D,E,F	Monotonic	8	8	CSP	12.5	4/12
32 – A,B,C	CUREE	8	8	CSP	12.5	4/12
33 – A,B,C	Monotonic	8	8	CSP	12.5	3/12
34 – A,B,C,D	CUREE	8	8	CSP	12.5	3/12

<sup>1</sup>Reversed cyclic test to determine first major event for Sequential Phase Displacement (SPD) tests

<sup>2</sup>Sequential Phase Displacement (SPD) reversed cyclic protocol

<sup>3</sup>CUREE reversed cyclic protocol for ordinary ground motions

<sup>4</sup>Fastener schedule (e.g. 3"/12") refers to the spacing between sheathing to framing screws around the edge of the panel and along intermediate studs (field spacing), respectively.

- i) Wall sheathing on one side only, oriented vertically (strength axis or face grain parallel to framing), consisting of either 12.5 mm CSA O151 Canadian Softwood Plywood (CSP) sheathing [3], 12.5 mm CSA O121 Douglas Fir Plywood (DFP) sheathing [2] or 11 mm CSA O325 Oriented Strand Board (OSB) sheathing [4] rated 1R24/2F16/W24.
- ii) 3-5/8" × 1-5/8" × 1/2" (92.1 × 41.3 × 12.7 mm) light gauge steel studs and 3-5/8" × 1-3/16" (92.1 × 30.2 mm) light gauge steel tracks manufactured in Canada to ASTM A653 [5] with nominal grade and thickness of 230 MPa and 1.12 mm, respectively. Studs were spaced at 24" (610 mm) on centre.



**Figure 1: Test frame with 4' x 8' (1220 × 2440 mm) wall specimen**

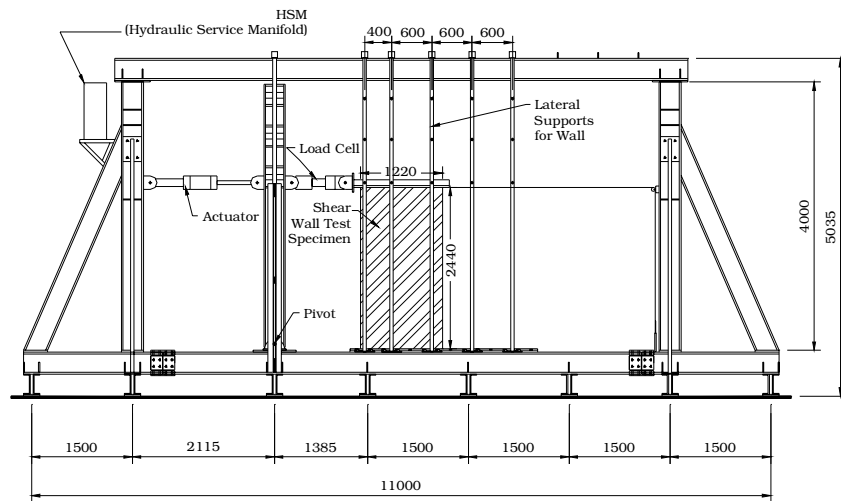


**Figure 2: Schematic of test frame with 4' x 8' (1220 × 2440 mm) wall specimen**

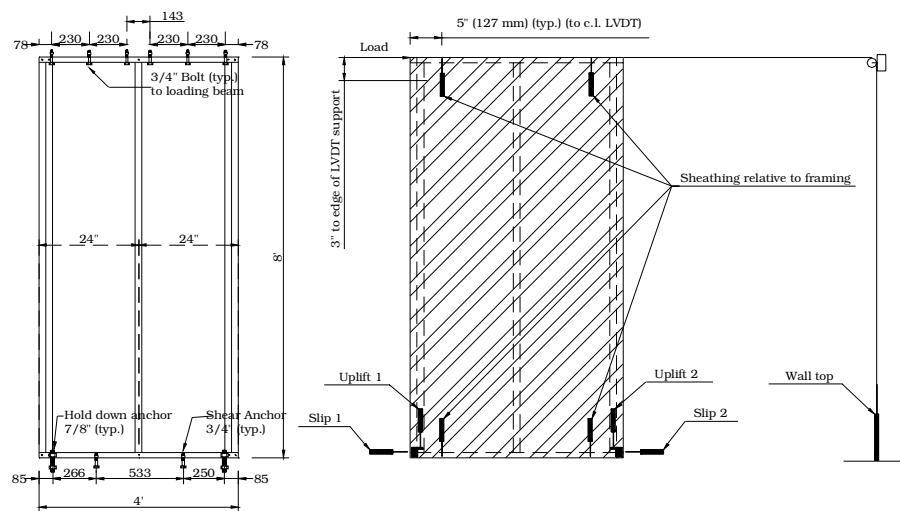


**Figure 3: Anchorage details and positioning of LVDTs for 4' x 8' (1220 × 2440 mm) wall specimens**

- iii) Back-to-back chord studs connected by two No. 10 × 3/4" (19.1 mm) long Hex washer head self-drilling screws at 12" (305 mm) on centre. The built-up member was incorporated in the wall framing in order to avoid both flexural and local buckling failure of a single chord stud on its own.
- iv) Simpson Strong-Tie S/HD10 [10] hold-down connectors attached to the chord studs with 33 No. 10 × 3/4" (19.1 mm) long Hex washer head self-drilling screws. An ASTM A307 [11] 7/8" (22.2 mm) diameter threaded anchor rod used to fasten each hold-down to the test frame (Figure 3).
- v) 3/4" (19.1 mm) diameter ASTM A325 bolts [12] used as shear anchors (Figure 3).
- vi) No. 8 × 1/2" (12.7 mm) long wafer head self-drilling framing screws to connect the track and studs.
- vii) No. 8 × 1-1/2" (38.1 mm) long Grabber SuperDrive [13] bugle head self-piercing sheathing screws installed at a distance of 1/2" (12.7 mm) from the edge of each sheathing panel. Panel edge screw spacing was 3" (76.2 mm), 4" (101.6 mm) or 6" (152.4 mm). Field screw spacing was 12" (304 mm).

## Loading Protocols

### Monotonic Tests

In order to simulate a “static” type loading, such as assumed in design for the case of wind loads on a building, and to establish the reversed cyclic loading protocols, monotonic tests were carried out following an identical procedure to that used by Serrette *et al.* [14]. The unidirectional displacement at the top of the wall was constant at a rate of 7.5 mm per minute starting from the zero force position. The test continued until a significant drop in load carrying capacity was observed. In an attempt to evaluate the permanent set at 12.5 mm and 38 mm, each wall specimen was unloaded when these displacements had been attained. Once the force in the wall reached zero, loading of the specimen recommenced. A wall resistance vs. deflection curve for a typical monotonic test is shown in Figure 4.

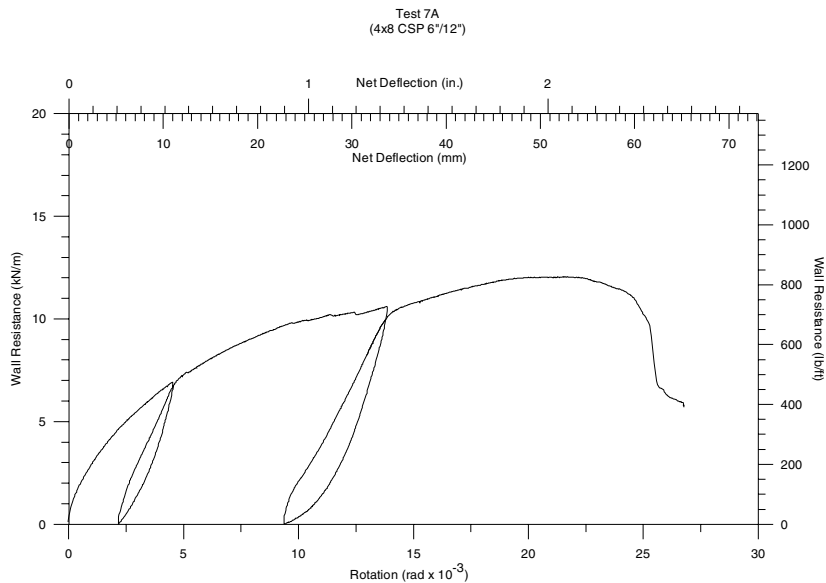


**Figure 4: Wall resistance vs. deflection curve for a typical monotonic test**

### Reversed Cyclic Tests

Prior to beginning the full suite of cyclic tests four series of the same wall configuration (specimens 1-A,B,C; 2; 3-A,B,C; 4-A,B,C) were tested in order to evaluate the feasibility of using the Sequential Phase Displacement (SPD) [15] or the CUREE [1] reversed cyclic loading protocols. Based on a study of these two protocols and on the results of these ten tests, the CUREE protocol for ordinary ground motions was found to be more suitable for the testing of steel frame / wood panel shear wall specimens [8]. The CUREE protocol was developed from the results of nonlinear dynamic time history analyses of structures

constructed of wood frame shear walls, and hence, in comparison to the SPD protocol, was considered to be more representative of the demand that would be imposed on the steel frame / wood panel shear wall building component during an earthquake. The protocol was also developed with the notion that multiple earthquakes may occur during the lifetime of the structure and subjects components to ordinary ground motions (not near-fault) whose probability of exceedance in 50 years is 10%. The loading protocol can affect the performance of a test wall, and hence influence the design values obtained from test results. This being said, it is important that the loading protocol reflects as much as possible the expected demand in a design level earthquake that may occur during the lifetime of a structure.

The loading history for the CUREE ordinary ground motions protocol is based on the average deformation capacity of three related monotonic tests. The monotonic deformation capacity,  $\Delta_m$ , is a post-peak deflection defined as the position at which the wall resistance is reduced to 80% of the maximum (peak) resistance. In order to define the maximum deflection that the wall will sustain during a reversed cyclic test, a certain fraction of  $\Delta_m$ , i.e.  $\gamma\Delta_m = 0.6\Delta_m$ , is used as a reference deformation,  $\Delta$ . The complete loading history, including the initiation, primary, and trailing cycles, is then based upon fractions of this reference deformation. The reversed cyclic tests were conducted at a frequency of 0.5 Hz and slowed to 0.25 Hz when the displacement amplitude exceeded 100 mm. An example loading history demonstrating the sequence of cycles is shown in Figure 5 and an example shear resistance vs. deflection hysteresis is provided in Figure 6.

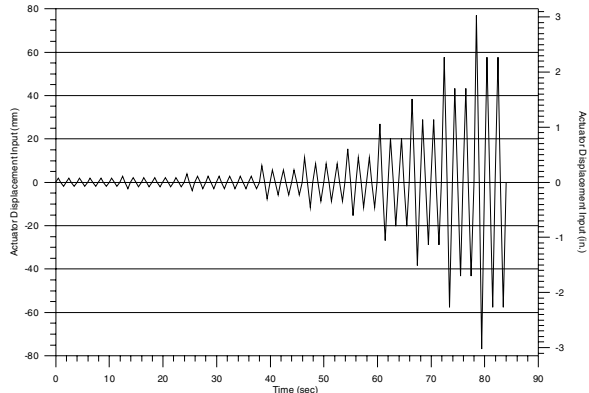


**Figure 5: CUREE ordinary ground motions protocol for shear wall tests 22-A,B,C**

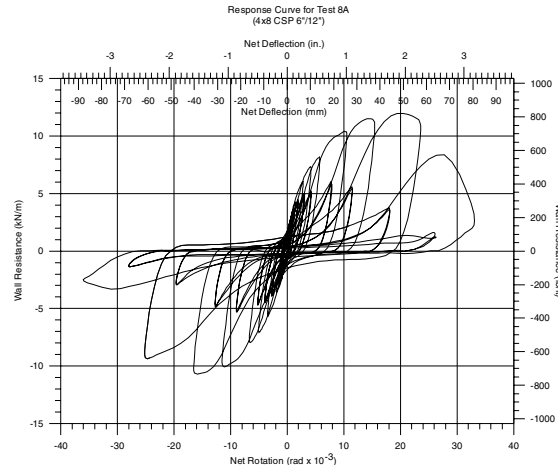


**Figure 6: Typical wall resistance vs. deflection curve for a reversed cyclic test**

## TEST RESULTS

### Behaviour of Shear walls

In general, the shear walls showed a non-linear behaviour from the onset of loading. Measurable permanent set was obtained at both the 12.5 mm and 38 mm displacement levels during the monotonic tests. This behaviour and ultimately the failure of almost all wall specimens were due to the deterioration or the complete loss of the connection between the sheathing panel and the light gauge steel framing. The failure modes for the wood to steel connections were classified into four main categories as follows: i) Partial or full pullout of the screws through the sheathing, ii) Tear out of the screws along the panel edge, iii) Bearing failure of the wood plies or strands, and iv) Combinations of these modes. In no case did a screw pull out of the flange of the steel studs or tracks. The hold-downs, the hold-down anchors, the shear anchors, and the steel-to-steel screw framing connections did not suffer any type of permanent damage. In some cases where the sheathing screw penetrated through two layers of steel, i.e. at the track to stud connection location, shear failure of the screw took place.

This type of failure was mainly due to the two layers of steel that allowed for less tilting of the screw, which resulted in greater shear force on the fastener and ultimately caused it to fail in shear. In the single steel layer case, the screw was allowed to tilt, and hence was mainly loaded in tension instead of shear. Higher connection forces could then be carried because of the screw material's superior tensile capacity. When the walls were subjected to reversed cyclic loading, fatigue of the sheathing connections may also have added to deterioration of the measured wall shear resistance.

The overall performance of a shear wall was governed by the sheathing connections. A sudden decline in wall capacity could be attributed to a complete side or the top or bottom of the panel being torn away or pulled away from the steel framing with the connections becoming no longer useful. The field fasteners rarely exhibited any type of damage. At times, after the ultimate load had been reached and failure had occurred over a large number of fasteners along the wall perimeter, the studs would act as short beams bending about their weak axis in order to transfer load. Local buckling of the studs would then occur in the flanges and return lips, however, since this behaviour occurred after the peak load had been reached it was not considered as a governing failure mode for the tests. In reality, this could cause significant problems if a gravity load had been in place. The compression chord studs would then be unsupported over a finite distance and would have developed a local buckle, which would cause their compression capacity to reduce depending on the unbraced length. In only one case (monotonic tests 13-A,B,C) did severe compression chord local buckling control the capacity of the wall. This wall configuration is characterized by Douglas Fir Plywood sheathing with a screw spacing of 3" (76.2 mm) around the perimeter of the panel. Because of the dense fastener schedule and the increased bearing resistance of the DFP adding to the overall strength of the shear wall, large compression forces developed in the chord studs. These compression forces caused local buckling in the webs, flanges and lips of the back-to-back studs. Compression chord buckling is an unfavourable governing failure mode for lateral force resisting shear walls because, in almost all cases, in addition to resisting a lateral load, the wall also supports gravity loads. It should be noted that the matching reversed cyclic tests (14-A,B,C,D) did not experience compression chord failure, rather the sheathing connections controlled the behaviour as for all other wall configurations.

### Comparison of Test Results

An overview of the direct results obtained from the test specimens is shown in Tables 2 (monotonic tests) and 3 (reversed cyclic tests). In all cases average values are provided, where corrections to displacements (rotations) based on uplift and slip measurements, as well as to loads based on measured accelerations (reversed cyclic tests only) have been applied [7]. Values that are presented include the maximum shear resistance recorded,  $S_u$ , the corresponding displacement in mm,  $\Delta_{net,u}$ , and radians,  $\theta_{net,u}$ , as well as the post-peak displacement at 0.8  $S_u$ ,  $\Delta_{net,0.8u}$  and  $\theta_{net,0.8u}$ . For the cyclic tests these values are given for both the positive and negative ranges of displacement. The energy dissipated during testing is also listed; that is the area under the resistance vs. deflection curve for the monotonic tests, and within the hysteretic loops for the cyclic tests.

In terms of general observations the following were recorded: Shear capacities reached for the monotonic and cyclic tests (positive displacement region) were similar for any specific wall configuration. Overall, the shear capacity increased with a greater density of fasteners around the panel perimeter. Energy dissipation was measurably higher for the longer walls, as well it increased with the screw fastener density. The 6"/12" CSP 2', 4' and 8' walls have similar ultimate shear capacity (per m), however the 2' walls require twice the displacement to reach this level, where 6"/12" refers to the panel edge / panel field sheathing fastener spacing. The 4"/12" CSP 2', 4' and 8' walls were not as consistent with respect to the shear strength as the 6"/12" walls, although the capacities are in the same range. The 2' walls again required significant racking displacement prior to reaching their ultimate shear strength. The 3"/12" CSP specimens also exhibited similar strengths for the two wall lengths that were tested (4' and 8'). Comparing the 4' long walls, DFP panels provided a higher

shear capacity for the different screw spacing scenarios compared with the CSP and OSB walls. Furthermore, OSB walls had slightly lower capacities than measured for walls constructed of CSP panels in most cases, however it must be noted that the OSB panels were thinner.

**Table 2: Monotonic shear wall test results (Average values)**

Specimen	Max. Wall Resistance ( $S_u$ ) kN/m	Disp. at $S_u$ ( $\Delta_{net,u}$ ) mm	Disp. at 0.8 $S_u$ ( $\Delta_{net,0.8u}$ ) mm	Rotation at $S_u$ ( $\theta_{net,u}$ ) rad	Rotation at 0.8 $S_u$ ( $\theta_{net,0.8u}$ ) rad	Energy Dissipation ( $E$ ) Joules
1 – A,B,C	16.6	60.6	78.0	0.0249	0.0320	1200
5 – A,B,C,D	23.8	60.6	75.5	0.0249	0.0310	1619
7 – A,B,C	12.7	50.7	67.1	0.0208	0.0275	825
9 – A,B,C	25.1	61.0	70.0	0.0250	0.0287	1609
11 – A,B,C	16.0	54.8	69.6	0.0224	0.0285	1027
13 – A,B,C <sup>2</sup>	29.7	58.2	62.6	0.0239	0.0257	1600
15 – A,B,C	12.2	103.3	131.7 <sup>1</sup>	0.0424	0.0540 <sup>1</sup>	729 <sup>1</sup>
17 – A,B,C	18.0	107.0	130.4	0.0439	0.0535	1050
19 – A,B,C	12.5	78.4	99.3	0.0322	0.0407	600
21 – A,B,C	13.2	41.1	54.7	0.0168	0.0224	727
23 – A,B,C	19.3	39.5	49.5	0.0162	0.0203	938
25 – A,B,C	23.5	40.7	46.8	0.0167	0.0192	1019
27 – A,B,C	18.4	78.0	98.2	0.0320	0.0403	882
29 – A,B,C	13.6	50.5	67.1	0.0207	0.0275	1783
31 – A,B,C,D,E,F	20.5	55.6	67.5	0.0228	0.0277	2551
33 – A,B,C	26.3	64.1	79.5	0.0263	0.0326	3865

<sup>1</sup>Based on tests 15 – C and 15 – B, test 15 – A did not reach 0.8  $S_u$  due to limited actuator displacement

<sup>2</sup>Tests 13 – A,B,C governed by compression chord local buckling

**Table 3: Cyclic shear wall test results (Average values)**

Specimen	Max. Wall Resistance		Disp. at $S_u$		Rotation at $S_u$		Energy Dissipation ( $E$ ) Joules
	+ve cycle ( $S_{u+}$ ) kN/m	-ve cycle ( $S_{u-}$ ) kN/m	+ve cycle ( $\Delta_{net,u+}$ ) mm	-ve cycle ( $\Delta_{net,u-}$ ) mm	+ve cycle ( $\theta_{net,u+}$ ) rad	-ve cycle ( $\theta_{net,u-}$ ) rad	
3 – A,B,C <sup>1</sup>	13.9	-14.0	39.8	-37.4	0.0163	-0.0153	12229
4 – A,B,C	17.5	-15.3	56.8	-44.0	0.0233	-0.0181	4942
6 – A,B,C	22.6	-19.6	58.7	-44.2	0.0241	-0.0181	6533
8 – A,B,C	11.9	-10.6	50.6	-38.1	0.0207	-0.0156	3890
10 – A,B,C	26.2	-23.1	54.1	-42.4	0.0222	-0.0174	6946
12 – A,B,C	14.6	-13.4	51.5	-39.9	0.0211	-0.0163	4491
14 – A,B,C,D	29.7	-26.2	53.4	-52.1	0.0219	-0.0213	7498
16 – A,B,C	11.2	-10.3	84.7	-59.6	0.0347	-0.0245	2637
18 – A,B,C	17.2	-15.5	95.1	-72.6	0.0390	-0.0298	3906
20 – A,B,C	11.3	-10.0	78.1	-47.5	0.0320	-0.0195	2737
22 – A,B,C	11.7	-10.5	42.0	-30.2	0.0172	-0.0124	3082
24 – A,B,C	17.2	-15.7	37.3	-28.4	0.0153	-0.0116	3867
26 – A,B,C	23.5	-22.4	37.9	-31.3	0.0155	-0.0128	4759
28 – A,B,C	18.0	-15.9	80.1	-77.9	0.0328	-0.0319	4288
30 – A,B,C	13.3	-11.9	51.9	-38.8	0.0213	-0.0159	8957
32 – A,B,C	20.3	-17.7	53.8	-43.2	0.0221	-0.0177	11937
34 – A,B,C,D	28.6	-25.0	59.9	-46.1	0.0245	-0.0189	16243

<sup>1</sup>Tests 3 – A,B,C were run using the SPD protocol

There exists a noticeable difference in the cyclic test results between the negative and positive regions of the protocol. Typically, damage to the shear wall is extensive on the first excursion in the positive direction when the ultimate load is reached, and upon movement in the reverse direction this damage does not allow for the wall to reach its previous performance level.

## DEVELOPMENT OF DESIGN INFORMATION

### Approach to Test Results Interpretation

Based on a review of existing design methods for shear walls, as well as data interpretation procedures for non-linear testing, a choice was made to incorporate the Equivalent Energy Elastic-Plastic (EEEP) bilinear model for the evaluation of all monotonic and reversed cyclic tests [7]. This approach was selected because it is independent of any cyclic loading protocol, it can be used for walls that show non-linear behaviour, and because it has been commonly applied in the analysis of test data for other types of structural systems [16]. In the case of each cyclic test a backbone curve was constructed for both the positive and negative displacement ranges of the resistance vs. deflection hysteresis. Each curve enveloped all of the cycles in one half of the protocol, however its shape was controlled by the first cycle at any given displacement. The EEEP curve was then created based on an equivalent energy approach, as illustrated in Figure 7.

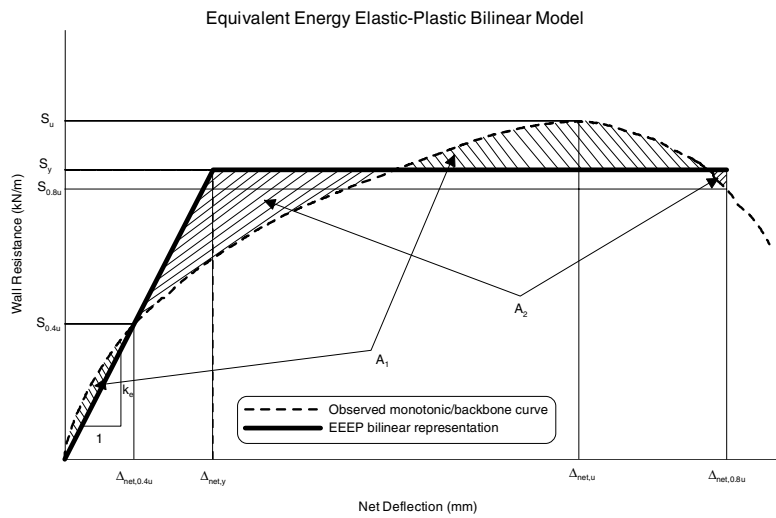


Figure 7: EEEP model

The EEEP curve for each reversed cyclic specimen was constructed by first determining three main parameters from the backbone curve, that is resistances:  $S_u$ ,  $S_{0.4u}$  and  $S_{0.8u}$  (post-peak), and all matching displacements:  $\Delta_{net,u}$ ,  $\Delta_{net,0.4u}$ , and  $\Delta_{net,0.8u}$  (post-peak) (Figure 7). Due to the non-linear behaviour of the walls, a straight line passing through the origin and the  $S_{0.4u}$  -  $\Delta_{net,0.4u}$  position was relied on to define the elastic portion and hence the stiffness,  $K_e$ , of the bilinear EEEP curve. The 40% resistance level was considered to be a reasonable estimate of the service load level. The area (energy) under the backbone curve was then calculated up to the post-peak displacement that corresponds to a wall resistance of  $S_{0.8u}$ . This load level was considered to be the limit of the useful capacity of each shear wall and represents the failure point of a specimen. A horizontal line depicting the plastic portion of the EEEP curve was then positioned so that the area bounded by the EEEP curve, the x-axis, and the limiting displacement,  $\Delta_{net,0.8u}$ , was equal to the area below the observed test curve. Or as shown in Figure 7, the areas  $A_1 = A_2$  were equated and the plastic portion of the bilinear curve was set as the wall shear yield resistance,  $S_y$ . This procedure was also followed for the negative displacements of the reversed cyclic tests. In addition, for each monotonic test the resistance vs. deflection curve (excluding the unloading portions) was interpreted

as a “backbone” curve, which allowed for the same EEEP bilinear curve to be drawn. Representative EEEP curves for the monotonic and reversed cyclic tests are shown in Figures 8 and 9, respectively.

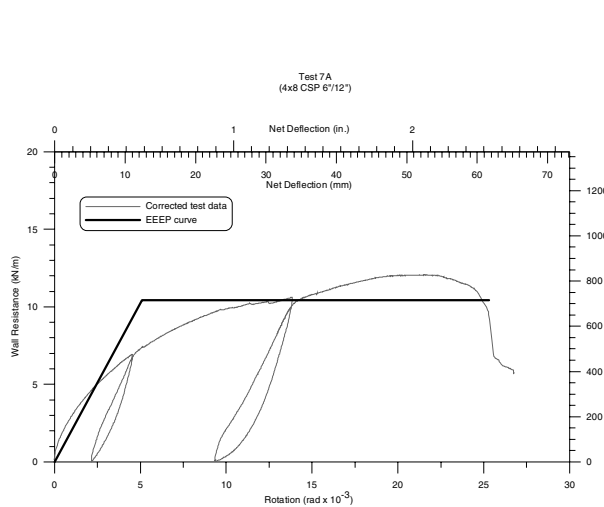


Figure 8: Monotonic EEEP curve

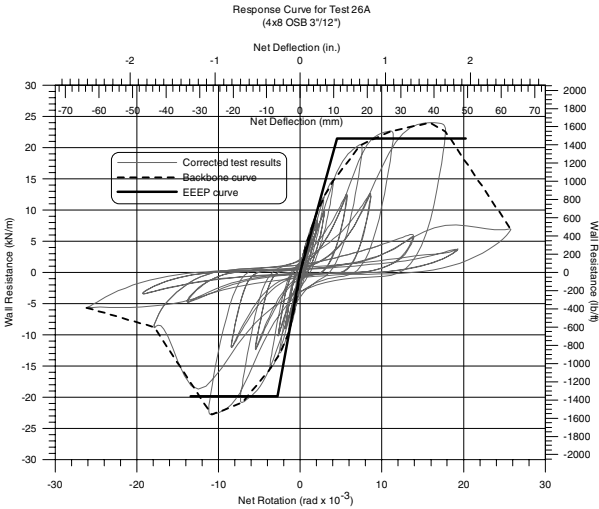


Figure 9: Reversed cyclic EEEP curve

### Inter-Storey Drift Limits

In the draft version of the 2005 National Building Code of Canada [6] a requirement exists that structural components be checked under the effect of service loads to ensure that both structural and non-structural elements, e.g. gypsum wall panels, will not be damaged in everyday performance of the building. The total drift per storey under service wind loads is limited to 1/500 of the storey height, in order to prevent cracking of the brittle interior finish. For a shear wall that is 8' (2440 mm) in height, an inter-storey drift limit of 4.9 mm is applicable. This measure was used to gauge the serviceability performance of light gauge steel frame / wood panel shear walls subjected to the monotonic loading protocol. The results of the data analysis demonstrated that for the 4' and 8' monotonic tests often the lateral deflection,  $\Delta_{net,0.4u}$ , at the serviceability load level for wind loads,  $S_{0.4u}$ , was in the 5 – 10 mm range. Typically, the 2' long walls resulted in the highest service level displacements. Additional research into the service level performance of these walls is necessary to properly address the use of a wind load based drift limit on design. Given the uncertainty that exists with respect to the service limit state of these walls, none of the design values shown in Tables 4, 5 and 6 were adjusted based on a service deflection limit.

The draft 2005 National Building Code of Canada also requires that for seismic design, lateral deflections obtained from a linear elastic analysis be multiplied by  $R_d R_o / I_E$  to estimate the inelastic response of the system, where  $R_d$  is the ductility related force modification factor,  $R_o$  is the overstrength related force modification factor, and  $I_E$  is the earthquake importance factor of the structure. For most structures intended for normal use the importance factor can be taken as unity. The largest inelastic inter-storey deflection is limited to 2.5% of the storey height for buildings of normal importance [6]. For an 8' (2440 mm) high shear wall this translates into an inelastic inter-storey drift limit of 61 mm. There are two cases (Figures 10&11) where the design of a light gauge steel frame / wood panel shear wall would be influenced by the inelastic drift limit of 61 mm: Case I:  $61 \text{ mm} < \Delta_{net,u}$  and Case II:  $\Delta_{net,u} < 61 \text{ mm} < \Delta_{net,0.8u}$ . A third case also exists in which the failure displacement of the test specimen at  $S_{0.8u}$  (post-peak) is below the seismic drift limit. In this situation, a restriction on the design capacity was not necessary and no modification to the EEEP curve procedure detailed above was utilized.

*Case I:  $61\text{mm} < \Delta_{\text{net},u}$*

In Case I, the 2.5% inelastic drift limit (61 mm) governs the capacity of the wall. For stability reasons, the shear wall specimen is considered to have failed when it reaches the inelastic drift limit. Unlike the serviceability deflection criteria explained above for wind loads, the seismic requirement is an ultimate limit state which must be respected in order to preserve the structural integrity of the overall building during and after a design level seismic event. In this case, the area under the backbone curve was calculated up to the displacement of 61 mm. The elastic portion of the bilinear EEEP curve was not affected by the imposed drift limit (it is still based on the secant stiffness through  $S_{0.4u}$ ), however, the horizontal plastic portion of the curve was adjusted so as to equate areas  $A_1$  and  $A_2$ , as illustrated in Figure 10. The imposed drift limit had the effect of slightly decreasing the shear yield resistance,  $S_y$ , as well as decreasing the ductility of the system,  $\mu$ , compared with an approach where no drift limit was imposed. Additionally, the force modification factors that are to be recommended for the design of these walls are based on this same EEEP approach and include the seismic inelastic drift limit [8]. Since the reduced ductility and shear yield resistance will be incorporated in the calculation of  $R$ -values from this test database, a designer would be able to use the given design capacity with confidence since, after calculating an elastic drift, and amplifying it by  $R_dR_o$ , it would still fall under the inelastic drift limit of 2.5% of the storey height. For consistency, this drift limit was also applied to all monotonic test data, even though reliance on this inelastic shear capacity during wind loading is typically not necessary. The Case I approach was followed for 31 wall specimens (19 monotonic and 12 cyclic tests).

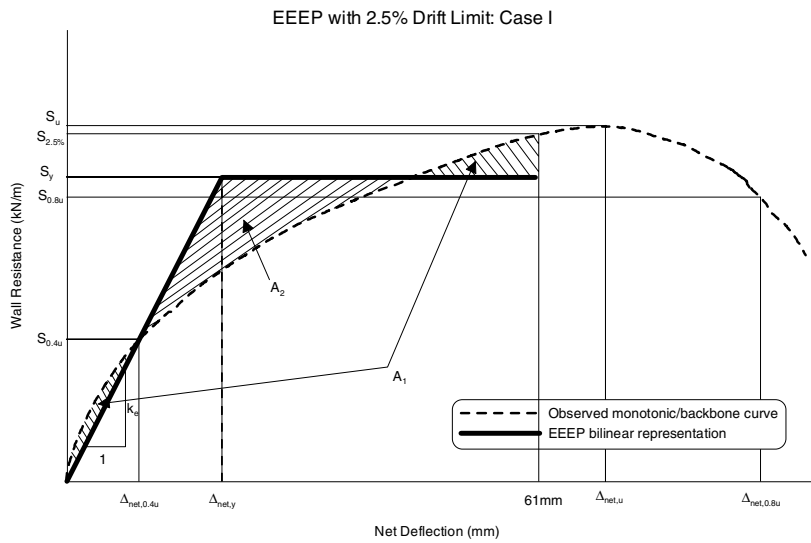


**Figure 10: EEEP design curve with imposed 2.5% drift limit (Case I)**

*Case II:  $\Delta_{\text{net},u} < 61\text{mm} < \Delta_{\text{net},0.8u}$*

In Case II, the ultimate resistance of the specimen occurred prior to reaching the 2.5% drift limit, although the  $S_{0.8u}$  post-peak load occurred at a displacement greater than 61 mm (Figure 11). In this situation the drift limit was not considered in determining the design values; instead the basic EEEP model was employed with failure defined at  $S_{0.8u}$ . In a design situation the computed inelastic drift would be compared with the NBCC limit and if found to be below this value then the wall would benefit slightly in terms of its design strength and ductility. The wall would be able to attain its maximum shear capacity prior to reaching the drift limit, and hence would develop the shear yield resistance as well. In an attempt to simplify the data interpretation procedure use of the drift limit was not considered necessary in this situation. It is possible that the wall will displace past the 2.5% drift limit during large excursions into the inelastic zone; however, the designer would be able to gauge the expected wall behaviour based on the inter-storey drift limit and select a stiffer wall configuration if required.

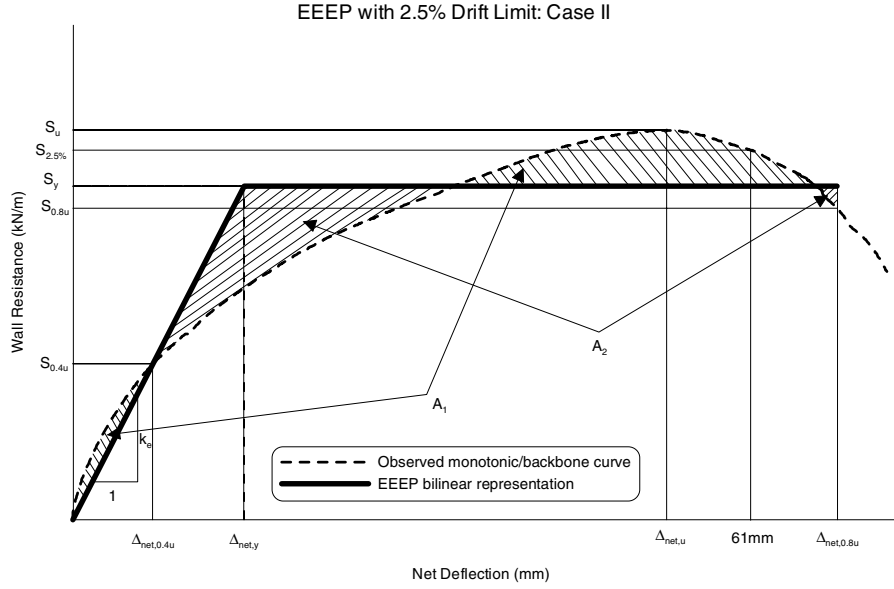


**Figure 11: EEEP design curve with imposed 2.5% drift limit (Case II)**

### Preliminary Values for Shear Wall Design

Design values for lateral loading of shear walls that are constructed in a similar fashion and with similar materials to those tested for this research are provided in Tables 4, 5 and 6. Included are average values for each monotonic and reversed cyclic test configuration based on the EEEP approach summarized above. Note that nominal values for the yield resistance (load),  $S_y$ , have been listed; which must be multiplied by an appropriate resistance factor for design. At this stage of the research project a corresponding resistance factor for limit states design following the NBCC has yet to be determined. In addition, the values listed are for lateral loading only; that is, there is no compensation applied to the design values for the possibility of compression chord failure under combined lateral and gravity loading.

**Table 4: Preliminary monotonic design values (Average values)**

Specimen	Yield Load ( $S_y$ ) kN/m	Disp. at $S_y$ ( $\Delta_{net,y}$ ) mm	Stiffness ( $K_e$ ) kN/mm	Rotation at $S_y$ ( $\theta_{net,y}$ ) rad	Ductility <sup>2</sup> ( $\mu$ )	Energy <sup>1</sup> Dissipation ( $E$ ) Joules
1 – A,B,C	14.2	19.0	0.92	0.0078	3.85	1101
5 – A,B,C,D	22.2	19.7	1.24	0.0081	3.43	1398
7 – A,B,C	11.1	13.0	1.05	0.0053	5.18	825
9 – A,B,C	21.5	19.7	1.33	0.0081	3.26	1426
11 – A,B,C	13.6	15.9	1.05	0.0065	4.39	1027
13 – A,B,C	24.7	18.9	1.59	0.0078	3.31	1600
15 – A,B,C	8.23	18.9	0.270	0.0077	3.26	258
17 – A,B,C	12.3	28.9	0.263	0.0118	2.12	348
19 – A,B,C	10.0	16.9	0.373	0.0069	3.70	321
21 – A,B,C	11.8	8.1	1.78	0.0033	6.76	727
23 – A,B,C	17.3	10.2	2.09	0.0042	4.88	938
25 – A,B,C	20.8	13.3	1.96	0.0054	3.58	1019
27 – A,B,C	14.9	15.9	0.570	0.0065	3.83	481
29 – A,B,C	11.9	11.6	2.520	0.0047	5.81	1783
31 – A,B,C,D,E,F	17.6	16.2	2.660	0.0066	4.17	2558
33 – A,B,C	21.6	19.1	2.760	0.0078	3.19	2707

<sup>1</sup>Energy dissipation determined under the backbone curve    <sup>2</sup> $\mu = \Delta_{failure} / \Delta_{net,y}$

**Table 5: Preliminary cyclic design values (Average positive values)**

Specimen	Yield Load ( $S_y$ ) kN/m	Disp. at $S_y$ ( $\Delta_{net,y}$ ) mm	Stiffness ( $K_e$ ) kN/mm	Rotation at $S_y$ ( $\theta_{net,y}$ ) rad	Ductility <sup>2</sup> ( $\mu$ )	Energy <sup>1</sup> Dissipation ( $E$ ) Joules
4 – A,B,C	15.5	14.9	1.28	0.0061	4.85	1211
6 – A,B,C	19.1	16.2	1.44	0.0067	4.21	1395
8 – A,B,C	10.5	10.1	1.26	0.0041	6.41	763
10 – A,B,C	22.6	17.3	1.61	0.0071	3.79	1551
12 – A,B,C	12.6	13.1	1.20	0.0054	5.02	890
14 – A,B,C,D	25.6	19.3	1.62	0.0079	3.51	1803
16 – A,B,C	8.63	22.6	0.240	0.0093	2.79	261
18 – A,B,C	12.7	27.0	0.287	0.0111	2.27	367
20 – A,B,C	9.29	16.1	0.363	0.0066	4.54	367
22 – A,B,C	10.7	7.5	1.75	0.0031	7.38	669
24 – A,B,C	15.5	8.1	2.34	0.0033	5.38	748
26 – A,B,C	20.8	10.6	2.41	0.0043	4.55	1091
28 – A,B,C	15.0	15.7	0.587	0.0064	3.90	480
30 – A,B,C	11.4	10.7	2.64	0.0044	6.01	1624
32 – A,B,C	17.5	15.7	2.72	0.0064	4.34	2563
34 – A,B,C,D	24.6	17.3	3.51	0.0071	4.01	3621

<sup>1</sup>Energy dissipation determined under the backbone curve   <sup>2</sup> $\mu = \Delta_{failure} / \Delta_{net,y}$

**Table 6: Preliminary cyclic design values (Average negative values)**

Specimen	Yield Load ( $S_y$ ) kN/m	Disp. at $S_y$ ( $\Delta_{net,y}$ ) mm	Stiffness ( $K_e$ ) kN/mm	Rotation at $S_y$ ( $\theta_{net,y}$ ) rad	Ductility <sup>2</sup> ( $\mu$ )	Energy <sup>1</sup> Dissipation ( $E$ ) Joules
4 – A,B,C	-13.6	-16.2	1.04	-0.0067	3.83	891
6 – A,B,C	-17.2	-15.5	1.36	-0.0063	4.08	1168
8 – A,B,C	-9.6	-12.3	0.96	-0.0051	4.72	614
10 – A,B,C	-20.7	-18.5	1.39	-0.0076	3.07	1155
12 – A,B,C	-11.7	-11.2	1.28	-0.0046	5.13	744
14 – A,B,C,D	-23.0	-15.5	1.82	-0.0063	4.05	1569
16 – A,B,C	-9.20	-15.8	0.353	-0.0065	4.44	353
18 – A,B,C	-12.4	-18.4	0.417	-0.0076	3.34	391
20 – A,B,C	-9.36	-12.8	0.470	-0.0052	6.33	424
22 – A,B,C	-9.6	-8.2	1.43	-0.0034	5.86	515
24 – A,B,C	-14.7	-8.8	2.04	-0.0036	4.62	640
26 – A,B,C	-20.1	-8.9	2.85	-0.0036	4.39	839
28 – A,B,C	-14.2	-15.9	0.547	-0.0065	4.68	585
30 – A,B,C	-11.5	-15.6	1.80	-0.0064	3.78	1440
32 – A,B,C	-16.5	-16.9	2.53	-0.0069	4.00	2277
34 – A,B,C,D	-22.2	-16.5	3.35	-0.0068	3.77	2909

<sup>1</sup>Energy dissipation determined under the backbone curve   <sup>2</sup> $\mu = \Delta_{failure} / \Delta_{net,y}$

The designer should be aware that the compression chord local buckling failure mode does exist and that it may control the maximum applied lateral load in the presence of gravity loads. Studies to determine a resistance factor for steel frame / wood panel shear walls and to quantify the effect of gravity loading on shear wall lateral performance are ongoing.

## CONCLUSIONS

Due to the lack in Canada of guidelines for engineers with which the design of laterally loaded steel frame / wood panel shear walls can be carried out an extensive research program has been undertaken at McGill University. The preliminary findings of 106 tests of shear walls constructed with Canadian wood sheathing and steel framing products were presented. Shear walls were tested monotonically, as well as with the CUREE ordinary ground motions reversed cyclic loading protocol. An overview of the direct results was provided, which indicated that given a specific wall configuration the 4' and 8' walls performed similarly, while the 2' walls required extensive lateral deformation to reach their ultimate shear capacity. Additionally, the shear capacity increased with the use of a smaller fastener spacing along the panel perimeter and with the use of DFP panels. An approach to interpret the shear wall test data that incorporates the Equivalent Energy Elastic-Plastic (EEEP) bilinear model was presented. Adaptations to this approach are necessary when the wall must exceed the 2.5% inter-storey seismic drift limit to reach its ultimate shear capacity. Nominal shear yield values were listed based on the EEEP approach, along with stiffness, ductility and energy measures. Additional research is needed to develop an appropriate resistance factor for limit states design and to evaluate the influence of gravity loads on lateral shear wall capacity. Furthermore, an investigation with respect to the wind service limit state drift limit should be completed.

## ACKNOWLEDGEMENTS

The authors would like to acknowledge the support provided by the Canada Foundation for Innovation, the Natural Sciences and Engineering Research Council of Canada, the Canadian Sheet Steel Building Institute, Simpson Strong-Tie Co. Inc., and the Canam Manac Group Inc.. Assistance with the procurement of steel framing was provided by Mr. John Rice of Bailey Metal Products Limited. A thank you is also extended to the undergraduate students: K. Hikita, D. Soulier, C.K. Hui and R.A. Lambert, who spent the summer of 2003 carrying out the shear wall tests in the structures laboratory at McGill University.

## REFERENCES

1. CUREE "Development of a Testing Protocol for Woodframe Structures", Consortium of Universities for Research in Earthquake Engineering, Pub. No. W-02, Richmond, CA, USA, 2001.
2. Canadian Standards Association O121. "Douglas Fir Plywood". Mississauga, Canada, 2001.
3. Canadian Standards Association O151. "Canadian Softwood Plywood". Mississauga, Canada, 2001.
4. Canadian Standards Association O325. "Construction Sheathing". Mississauga, Canada, 2001.
5. ASTM A653, "Standard Specification for Steel Sheet, Zinc-Coated (Galvanized) or Zinc-Iron Alloy-Coated (Galvannealed) by the Hot-Dip Process", West Conshohocken, USA, 2002.
6. National Research Council of Canada, Institute for Research In Construction. "Proposed changes to NBC 1995 – Part 4". Ottawa, Canada, 2001.
7. Branston, A.E., "Development of a Design Methodology for Steel Frame / Wood Panel Shear Walls", Master's Thesis, Dept. of Civil Engineering and Applied Mechanics, McGill University, Montreal, Canada, 2004.
8. Boudreault, F.A., "Seismic Analysis of Steel Frame / Wood Panel Shear Walls", Master's Thesis, Dept. of Civil Engineering and Applied Mechanics, McGill University, Montreal, Canada, 2004.
9. Chen, C.Y., "Testing and Performance of Steel Frame / Wood Panel Shear Walls", Master's Thesis, Dept. of Civil Engineering and Applied Mechanics, McGill University, Montreal, Canada, 2004.
10. Simpson Strong-Tie Co. Inc., "Light Gauge Steel Construction Connectors", Dublin, USA, 2001.
11. ASTM A307, "Standard Specification for Carbon Steel Bolts and Studs, 60000 psi Tensile Strength", West Conshohocken, USA, 2000.

12. ASTM A325, "Standard Specification for High-Strength Bolts for Structural Steel Joints", West Conshohocken, USA, 2002.
13. SuperDrive, "Grabber SuperDrive Construction Products", [www.superdrive.info](http://www.superdrive.info), 2003.
14. Serrette, R., Nguyen, H., Hall, G. "Shear Wall Values for Light Weight Steel Framing", Report No. LGSRG-3-96, Light Gauge Steel Research Group, Dept. of Civil Engineering, Santa Clara University, Santa Clara, USA, 1996.
15. Structural Engineers Association of Southern California. "Standard Method of Cyclic (reversed) Load Test for Shear Resistance of Framed Walls for Buildings", Whittier, USA, 1997.
16. Park, R. "Evaluation of Ductility of Structures and Structural Assemblages from Laboratory Testing", Bulletin of the New Zealand National Society for Earthquake Engineering, Vol. 22, No. 3, 1989.